BBA - Molecular and Cell Biology of Lipids 1866 (2021) 158928

Contents lists available at ScienceDirect

BBA - Molecular and Cell Biology of Lipids

journal homepage: www.elsevier.com/locate/bbalip

The key to the allergenicity of lipid transfer protein (LTP) ligands: A structural characterization

Zulema Gonzalez-Klein [a], Bruno Cuevas-Zuviria [a], Andrea Wangorsch [b], Guadalupe Hernandez-Ramirez [a], Diego Pazos-Castro [a], Carmen Oeo-Santos [c,d], Alejandro Romero-Sahagun [a], Luis F. Pacios [a], Jaime Tome-Amat [a], Stephan Scheurer [b], Araceli Diaz-Perales [a], María Garrido-Arandia [a,*]

[a] Centro de Biotecnología y Genómica de Plantas (UPM-INIA), Universidad Politécnica de Madrid, Pozuelo de Alarcón, Madrid, Spain
[b] Molecular Allergology, Paul-Ehrlich-Institut, Langen, Germany
[c] Departamento de Bioquímica y Biología Molecular, Facultad de Ciencias Químicas, Universidad Complutense de Madrid, Madrid, Spain
[d] Cellular Degradation Systems Laboratory, The Francis Crick Institute, London, United Kingdom

ARTICLE INFO

Keywords:
Food allergy
Lipid transfer protein
Ligand
Phytosphingosine

ABSTRACT

Plant lipid transfer proteins are a large family that can be found in all land plants. They have a hydrophobic cavity that allows them to harbor lipids and facilitates their traffic between membranes. However, in humans, this plant protein family is responsible for the main food allergies in the Mediterranean area. Nevertheless, not only the protein itself but also its ligand is relevant for allergic sensitization.

The main aim of the present work is to analyse the natural ligands carried by four allergenic LTPs (Tri a 14, Art v 3, Par j 2, and Ole e 7), compared with the previously identified ligand of Pru p 3 (CPT-PHS ligand), and clarify their role within the immunological reactions.

Results showed that the ligands of the LTPs studied shared a chemical identity, in which the presence of a polar head was essential to the protein-ligand binding. This ligand was transported through a skin cellular model, and phosphorylated phytosphingosine could be detected as result of cell metabolism. Since sphingosine kinase 1 was overexpressed in keratinocytes incubated with the LTP-ligand complex, this enzyme might be responsible for the phosphorylation of the phytosphingosine fraction of the CPT-PHS ligand. This way, phytosphingosine-1-phosphate could be mimicking the role of the human inflammatory mediator sphingosine-1-phosphate, explaining why LTPs are associated with more severe allergic responses. In conclusion, this work contributes to the understanding of the chemical nature and behavior of lipid ligands carried by allergens, which would help to gain insight into their role during allergic sensitization.

1. Introduction

Allergic reactions are estimated to affect more than 20% of the USA and Europe's population, and their prevalence is increasing [1]. They are the result of an immune response against innocuous environmental proteins [2]. However, the reason why a protein becomes an allergen is still unknown. Over 2000 allergenic proteins have been identified [3], but they belong to only 1% of the known protein families [4]. It must also be noted that not all members of these families are allergenic [5], so belonging to a specific protein family does not seem to be what determines their allergenicity.

It has been reported that more than 50% of plant allergens are lipid

Abbreviations: CPT, camptothecin; LTP, lipid transfer protein; MD, molecular dynamics; PC, phosphatidylcholine; PHS, phytosphingosine; PHS1P, phytosphingosine-1-phosphate; SPH, sphingosine; SphK1, sphingosine kinase 1; S1P, sphingosine-1-phosphate; TLC, thin-layer chromatography.

* Corresponding author at: Centre for Plant Biotechnology and Genomics (UPM-INIA), Universidad Politécnica de Madrid Pozuelo de Alarcón, 28223 Madrid, Spain.

E-mail addresses: zulema.gonzalez.klein@upm.es (Z. Gonzalez-Klein), bruno.czuviria@upm.es (B. Cuevas-Zuviria), Andrea.Wangorsch@pei.de (A. Wangorsch), guadalupe.hernandez@upm.es (G. Hernandez-Ramirez), d.pazosc@upm.es (D. Pazos-Castro), alejandro.romero.sahagun@upm.es (A. Romero-Sahagun), luis.fpacios@upm.es (L.F. Pacios), jaime.tome@upm.es (J. Tome-Amat), Stephan.Scheurer@pei.de (S. Scheurer), araceli.diaz@upm.es (A. Diaz-Perales), maria.garrido@upm.es (M. Garrido-Arandia).

https://doi.org/10.1016/j.bbalip.2021.158928
Received 14 January 2021; Received in revised form 15 March 2021; Accepted 20 March 2021
Available online 24 March 2021

carriers [4], and these ligands may act as adjuvants and skew the immune system towards a type 2 (pro-allergenic) response [6]. This kind of ligands has been described in allergens that belong to the Bet v 1 family [7,8], lipid transfer proteins (LTPs) [9], 2S albumins [10], globulins, vicilins [11] and lipocalins [12]. Among these protein families, LTPs contribute to either a primary food allergy or a pollen-food syndrome [13].

Non-specific lipid transfer protein 1 (nsLTP1) is a protein family of basic polypeptides of 9 kDa, widely distributed throughout the plant kingdom [14]. Despite the heterogeneity in their amino acid sequence, nsLTP1s share a high conserved compact fold, composed of four α-helices connected by short loops and a non-structured C-terminal tail. This fold, which is stabilized by four disulphide bridges, enables the formation of a hydrophobic tunnel-like cavity where ligands with long chains can be accommodated [15].

Different computational analyses and *in vitro* assays have demonstrated the plasticity of LTPs in their lipid-binding mechanism. The flexibility of their inner cavity seems to allow them to accommodate different kinds of lipids such as fatty acids, fatty acyl-CoA, phospholipids, glycolipids and hydroxylated fatty acids [16–18]. However, only the natural ligand transported by one LTP (the major peach allergen Pru p 3) has been characterized up to now. This ligand was identified as a derivative of the alkaloid camptothecin (OH-CPT) bound to a long hydrophobic tail of phytosphingosine (PHS) [9]. The essential role of LTP ligand as an adjuvant in the allergic sensitization process was also described [4].

Taking into account the immunomodulatory role of ligands carried by allergens, their identification is a key step to understand the allergic response. The types of ligands bound to allergens will depend on the structure of the proteins, but also on their biological function and their location at the time of binding. For that reason, the main goal of this work is the identification and comparison of natural ligands carried by four different allergenic LTPs to determine the *in vivo* selectivity and specificity of the LTP protein family. Besides that, *in vitro* assays were performed using liposomes, immunoassays, along with computational analyses, in order to determine the binding affinity and interaction mode of the protein-ligand complexes. In addition, this work aims to deepen into the immunological role of the ligands of allergenic LTPs. These goals would help us to understand the role of lipid ligands in the allergic sensitization process.

2. Material and methods

2.1. Sequence and structural alignment

Amino acid sequences of four of the selected LTPs were obtained from UniProt database: Pru p 3 (P81402), Tri a 14 (P24296), Art v 3 (C4MGG9), and Par j 2 (P55958) [19], while that of Ole e 7 was kindly provided by Dr. M. Villalba (Department of Biochemistry and Molecular Biology, Universidad Complutense de Madrid). Sequence identities among all these LTPs were based upon Clustal 2.1 pairwise alignments using Clustal Omega tool [20]. Secondary structure prediction was performed using the PSIPRED server [21].

Experimental structures of Pru p 3 and Tri a 14, with PDB entries 2B5S [22] and 1BWO [23] respectively, were used for structural comparison analysis. Structures of Art v 3, Par j 2, and Ole e 7 were obtained by homology modelling using the Swiss-Model server (https://swissmodel.expasy.org/) [24,25]. Structural superpositions were computed and analysed using Chimera software (http://www.rbvi.ucsf.edu/chimera) [26] and cavities were detected with the DogSite method implemented in the Proteins Plus server (http://proteinsplus.zbh.uni-hamburg.de/#dogsite) [27].

2.2. Isolation of proteins

Selected LTPs were purified from peach peel (*Prunus persica*), wheat bran (*Triticum aestivum*), mugwort pollen (*Artemisia vulgaris*), pellitory pollen (*Parietaria judaica*), and olive pollen (*Olea europaea*) as previously described [28], and their identities were confirmed by immunodetection with specific anti-LTP antibodies (provided by Carlos Pastor, Hospital Universitario Fundación Jiménez Díaz, Madrid, Spain).

Recombinant Pru p 3 (rPru p 3) was produced in *Pichia pastoris* as previously described [28]. The purity and identity of the protein were confirmed by MALDI-TOF (UltraFlex II, Bruker Daltonics, Germany) analysis at the Research Support Center of the Universidad Complutense de Madrid using sinapinic acid as matrix. The absence of molecules bound to its hydrophobic cavity was verified using the transfected cell line THP1-XBlue™ (Invivogen, France).

2.3. Ligands isolation from allergenic LTPs

The presence of the ligands in the retained fraction obtained after cationic exchange chromatography was confirmed by thin-layer chromatography (TLC) on silica gel–coated plates (Merck, USA) developed with ethanol: acetic acid: ethyl acetate (6:3:1) in a saturated chromatography chamber. The plates were visualized under UV light (254 nm) and stained with vanillin (1% in ethanol) (Sigma-Aldrich, Germany).

Ligands were isolated and purified by size-exclusion LH-20 chromatography (GE Healthcare Sephadex™ LH-20, Fisher Scientific), as previously described [9]. They were quantified by absorbance at 254 nm, using commercial OH-CPT (Sigma-Aldrich) as standard. The presence of protein contamination in ligand samples was discarded by immunodetection on a nitrocellulose membrane (Amersham™ Hybond ECL, Nitrocellulose Blotting Membrane, GE Healthcare) using specific antibodies against LTP and recombinant Pru p 3 as a positive control.

2.4. Characterization of ligands

Characterization assays described for the identification of the ligand of Pru p 3 [9] were carried out with all the LTP ligands. Elution profiles by reversed-phase high-performance liquid chromatography were compared. The presence of a camptothecin-like polar group in the ligands was confirmed by its capacity of emission under UV (365 nm) on silica gel-coated plates, and its ability to inhibit topoisomerase I (Inspiralis, UK) activity, as previously reported [9].

Besides that, the presence of a PHS tail was studied using the transfected cell line THP1-XBlue™ (Invivogen) as previously described [4]. The results were expressed as stimulation index (SI), calculated as the ratio between the absorbance values of the stimulated cells and the absorbance value of the negative control. Stimulation indexes above the negative control value +3SD were considered positive.

2.5. Ligand identification by mass spectrometry

Ligands were identified by mass spectrometry in the Research Support Center of the Universidad Complutense de Madrid. Ligands were solubilized in LC/MS quality methanol and injected with acetonitrile: water (1:1) and 0.1% formic acid as mobile phase with a flow rate of 0,5 mL/min. The analysis was performed in a triple quadrupole LC-MS 8030 (Shimadzu, Japan). The following settings were applied: 2 min analysis in Q3 scan mode; misting gas flow, 1 L/min; dry gas flow, 10 L/min; dry gas temperature, 250 °C; interphase voltage, 3.5 kV; and detector voltage, 1.84 kV. Samples were analysed in ESI+ mode.

2.6. Production and characterization of the synthetic CPT-PHS ligand

The synthesis of the molecule previously described as the natural ligand of Pru p 3 was accomplished through the chemical formation of an amide bond between two commercial compounds: OH-CPT and PHS (Sigma-Aldrich). Briefly, an equimolar mixture of both compounds was incubated with 0.25 mM N-Hydroxysuccinimide (NHS, Sigma-Aldrich) and 0.1 mM EDC (Sigma-Aldrich) in MES buffer 50 mM (Sigma-

Aldrich) 0.1% Tween® 20 (Sigma-Aldrich) overnight at 4 °C.

The synthetic CPT-PHS ligand was purified by high-performance liquid chromatography using a Nucleosil 120-C18 column (5 μm 250×4mm, Scharlab) with an isocratic method in acetonitrile: water (85:15) at a flow rate of 0.5 mL/min for 70 min. Sample peaks were detected using absorbance at 254 nm. The identity of the ligand was confirmed by its elution profile in HPLC, its capacity to emit under UV light (365 nm) and to activate the NF-kB pathway, as described above for the natural ligands included in Section 2.5 of materials and methods. Furthermore, the stability of the complex (Pru p 3 + synthetic CPT-PHS) was compared with that of Pru p 3 complexed with its natural CPT-PHS ligand using nano differential scanning fluorimetry as explained in Section 2.9 pf materials and methods.

2.7. Membrane model binding assay

To trace the binding of lipids to Pru p 3, all molecules were labelled with different fluorophores according to the manufacturer's instructions. PHS (Sigma-Aldrich) was labelled with Alexa 488 (Alexa Fluor™ 488 NHS Ester, Thermo Fisher, USA) and selected fatty acids (oleic, linoleic, and stearic acid purchased from Sigma-Aldrich) were labelled with Alexa 488 (Alexa Fluor™ 488 Cadaverine, Thermo Fisher). rPru p 3 was labelled with Alexa 647 (Alexa Fluor™ 647 NHS Ester, Thermo Fisher).

Liposomes production protocol was based on Akbarzadeh et al. (2013) with modifications [29]. Briefly, phosphatidylcholine (PC) and selected lipids (13:1 proportion) were solubilized in chloroform: methanol (1:1) and lyophilized to create a lipidic thin layer. Lipids were put in contact with ammonium acetate 0.1 M and shaken with a vortex every 10 min for an hour. Once the liposomes were formed, they were washed three times with ammonium acetate 0.1 M through centrifugation (10 min, 12.000 g). The proper formation of liposomes was confirmed by contrast phase microscopy (Leica TCS-SP8, Germany).

To study the binding of Pru p 3, different liposomes were incubated with labelled Pru p 3 in agitation for 2 h at RT. After several washes with ammonium acetate 0.1 M, the binding of Pru p 3 was studied by flow cytometry (BD Accuri™ C6 Cytometer, BD Biosciences, USA). Labelled lipids and Pru p 3 were traced using a laser excitation wavelength of 488 nm and 640 nm, respectively. The emission was detected by the optical filters FL1 533/30 nm and FL4 675/25 nm, and 100.000 events were collected in all the experiments. Co-localization and homogeneity of liposomes were visualized by confocal microscopy (Leica TCS-SP8) using the 488 nm and 633 nm laser excitation and 63× objective.

2.8. Experimental determination of protein-ligand binding affinities

The affinity of Pru p 3 for different lipid-ligands was studied using Polysorp Nunc-Immunoplates (Thermo Scientific, Denmark) as previously described with modifications [30]. The plates were coated with 2,5μg/well of CPT-PHS ligand, PHS, oleic, linoleic, or stearic acid respectively, dissolved in methanol. Pru p 3 was incubated at different concentrations (31.3, 15.6, 7.8, 3.9, 1.9, 0.98, 0.49, 0 μg/mL) in PBS for 3 h at 37 °C. Specific antibodies against Pru p 3 and horseradish peroxidase (HRP)-conjugated anti-rabbit secondary antibodies were used for the detection of bound protein. Absorbance values of three independent experiments were fit to a curve with non-linear regression using One site – Specific binding equation in GraphPad Prism version 6.01 for Windows (GraphPad Software, San Diego, California, USA) to calculate a Kd value for each ligand.

2.9. Thermal stability assays

Nano differential scanning calorimetry (nanoDSF) experiments were carried out using the Prometheus NT.48 instrument (NanoTemper Technologies, Germany). Melting temperatures (Tm) of Pru p 3 alone and complexed with different ligands (sCPT-PHS ligand, PHS, CPT, oleic, linoleic, and stearic acid) were determined. The capillaries were filled with 10 μL sample consisting of a mixture of Pru p 3 at 50 μM in PBS and the ligand in each case at 200 μM in dimethyl sulfoxide. A temperature gradient of 2.0 °C/min from 20 to 110 °C was applied and the intrinsic protein fluorescence at 330 and 350 nm was recorded. The fluorescence intensity ratio and its first derivative were calculated with the manufacturer's software (PR.ThermControl) in order to obtain the unfolding transition temperature (Tm).

2.10. Molecular-dynamics simulations

The affinity of Pru p 3 for six different ligands was simulated using umbrella sampling. This technique is widely employed to study the energy changes of different phenomena [31]. In this case, the energy differences between bound and unbound states were compared. The initial conformation for Pru p 3 was retrieved from the entry 2ALG of the Protein Data Bank (PDB) [22]. The structures of the ligands were modelled using Chimera [26] and the protein-ligand docking software AutoDock-Vina [32] was used to obtain the geometries of the ligands docked into the protein cavity. The CHARMM-GUI portal [33] provided the simulation set-ups (topology files, parameters, solvation, etc) for the molecular dynamics (MD) calculations. MD simulations were carried out using the CHARMM36 force field [33] [34] implemented in NAMD2.14 [35] combined with the collective variables module COLVARS [36]. Previously to the umbrella-sampling protocol, a 10 ns MD simulation relaxed the protein-ligand system and avoided docking artefacts. The umbrella sampling protocol consisted of moving the constraint along 21 equally spaced steps to pull out the ligand from the binding site. The force of the constraints was 3.33 kcal/mol/Å^2. The umbrella sampling step lasted 42 ns. The output of the simulations (distances to restraint centre) was analysed using the weighted histogram analysis method (WHAM) [37,38].

2.11. Ligand cleavage

A431 cells (ATCC® CRL-1555TM; human epidermal keratinocytes) were seeded in coverslips in supplemented DMEM (Lonza, Switzerland) and were incubated with 20 μg/mL of complex (rPru p 3 + CPT-PHS ligand (10:1)), 2 μg/mL of CPT-PHS ligand, 2 μg/mL of PHS or 2 μg/mL of OH-CPT for 48 h. After washing, they were fixed for 10 min with 4% PFA and stained with DAPI. Specimens were mounted with ProLong™ Gold (Invitrogen) and images were obtained by confocal microscopy (Zeiss LSM 880, USA).

2.12. In vitro skin cellular model

An *in vitro* skin cellular model was designed to mimic the skin mucosa. 24-well Transwell® culture plates (0.4 μm pore diameter; Corning® Inc., Sigma-Aldrich) were treated with collagen from human placenta (Sigma-Aldrich) and seeded with 6×10^3 BJ cells (ATCC® CRL-2522™; human fibroblasts). Cells were seeded in the Transwell® membrane but oriented towards the basolateral chamber. After 24 h of culture, 1×10^5 A431 cells were seeded onto the apical chamber and grown O/N. After that, cells were cultured on airlift for 96 h. Supplemented DMEM (Lonza, Basel, Switzerland) was used as the culture medium. The permeability of the skin epithelium was evaluated by fluorescein transport as previously described for other epithelial monolayers [39].

To determine whether Pru p 3 and its CPT-PHS ligand could be transported or metabolized by the epidermal epithelium, complex (1 μg) was added to the apical side of the Transwell®. Basolateral medium was substituted by Hank's Balanced Salt Solution (Lonza) and samples were collected after 10, 20, 60, 90, 120, and 240 min. The amount of Pru p 3 in these media was measured by ELISA, coating 96-well microtiter plaques (Corning® Costar®, Sigma-Aldrich) with the basolateral samples and using specific antibodies. Basolateral samples were also

collected after five days of incubation with complex in supplemented DMEM media, and analysed to determine its lipid profile by ESI-QQQ-MS (LC-MS 8030, Shimadzu, Japan) in the Universidad Complutense de Madrid, after performing a metabolite extraction as previously described [40].

2.13. RNA isolation and RT-qPCR

A431 cells were seeded in 24-well plates in supplemented DMEM and were incubated with 20 μg/mL of complex for 72 h. Cells were lysed and homogenized with GIT extraction buffer (pH = 7; 4 M guanidine isothiocyanate (Sigma-Aldrich); 25 mM sodium citrate (Sigma-Aldrich); 0.5% sarcosyl (Sigma-Aldrich); 0.1 M 2-mercaptoethanol (Carl Roth, Germany)). RNA was purified by phenol: chloroform extraction and precipitated with ethanol. Its purity and concentration were assessed using a spectrophotometer (NanoDropTM, ThermoFisher).

cDNA was obtained with the High-Capacity cDNA Reverse Transcription Kit (ThermoFisher), following the provider's instructions. qPCR was performed using the FastStart Universal SYBR Green Master (Roche, Switzerland) and specific oligonucleotides for sphingosine kinase 1 (SphK1; Forward: GCTGGCAGCTTCCTTGAACCAT; Reverse: GTGTGCAGAGACAGCAGGTTCA) and GAPDH (Forward: GAGTCAAACGGATTTGGTCGT; Reverse: TTGATTTTGGAGGGATCTCG). GAPDH was used as an endogenous gene to normalize the results. Relative expression of the treated sample for each gene was referred to the untreated one.

2.14. Colocalization of complex with SphK1

A431 cells were incubated with 0.5 μg of complex for 10 min RT. After washing, they were fixed for 10 min with 4% PFA and stained with DAPI. Blocking was performed with Casein Blocking Buffer (Sigma-Aldrich) for 1 h RT. Specific antibodies against Pru p 3 (1:300) and SphK1 (1:1000, G Biosciences, USA) were added for 1 h RT. After washing, Alexa Fluor-labelled antibodies (Hospital Puerta de Hierro, Spain) were added for an additional hour. Specimens were mounted with ProLong™ Gold (Invitrogen) and images were obtained by confocal microscopy (Zeiss LSM 880).

2.15. In vitro phytosphingosine phosphorylation assay

To study the capacity of the human SphK1 to phosphorylate the CPT-PHS ligand, PHS was incubated with SphK1 (2 U; SRP0283, Sigma-Aldrich) in Mg^{2+} containing buffer pH = 7.5 with an excess of ATP (adenosine 5′-triphosphate disodium salt hydrate, Sigma-Aldrich). The reaction was performed O/N at 37 °C. The product was analysed by MALDI-TOF (UltraFlex II, Bruker Daltonics) in the Universidad Complutense de Madrid, with a laser model LTB MNL 106. 2.5-dihydroxybenzoic acid was used as matrix.

2.1. Migration assay

The biological activity of phytosphingosine-1-phosphate (PHS1P) as chemoattractant was evaluated performing a monocyte migration assay as previously described with modifications [41]. 10^5 THP-1 monocyte-like cells were seeded in 24-well Transwell® culture plates (8 μm pore diameter; Falcon®, Corning® Inc.). 40 nM of PHS (Sigma-Aldrich) and PHS1P (Avanti Polar Lipids, USA) were added to RPMI medium (Lonza) in the basolateral chamber. Sphingosine-1-phosphate (S1P; Avanti Polar Lipids) was used as positive control and RPMI medium alone as negative control. The percentage of cell migration with different stimuli was calculated with the cells counted in the basolateral chamber after 6 h of incubation using a cytometer (BD Accuri™ C6 Cytometer, BD Biosciences).

2.16. Statistical analyses

Statistically significant differences were analysed by GraphPad Prism version 6.01 using the Kruskal-Wallis test with Dunn's correction for multiple comparisons and the Mann-Whitney test. *P*-values <0.05 were considered significant.

3. Results

3.1. Five selected allergenic LTPs show higher structural than sequence similarity

To study the nature of the ligands transported by LTPs, five allergenic nsLTPs were selected: Tri a 14 *(Triticum aestivum),* Art v 3 *(Artemisa vulgaris)*, Par j 2 *(Parietaria judaica)*, Ole e 7 *(Olea europea),* and Pru p 3 *(Prunus persica)* as reference. Although the studied LTPs have sequence identities between 24.7% and 51.1% (Fig. 1A), some residues with a role in lipid binding, such as Arg44 and Tyr79 [21], are conserved. Arg44 is conserved in Tri a 14 and Art v 3, while it is substituted by another basic amino acid (Lys) in Par j 2 and Ole e 7. Likewise, Tyr79 is conserved in Tri a 14 (Tyr78) and Art v 3 (Tyr79), while it is replaced by Leu in both Par j 2 (Leu81) and Ole e 7 (Leu82). Other amino acids known to specifically interact with the ligand of Pru p 3 are Leu10, Ile14, Val17, Leu 51, Leu54, Ser55, and Ala 66 [34]. They are mostly conserved or substituted by equivalent amino acids in the other LTPs investigated.

On the other hand, the structural alignment showed higher similarities than the sequence alignment. The secondary structure was predicted from sequence and it revealed the presence of four helices located in the same amino acid region for all the LTPs studied. Moreover, the tridimensional structure showed that this fold is stabilized by four disulphide bridges and it could be detected the non-structured long C-terminal tail (Fig. 1B). The analysis of the internal cavity of these proteins revealed the presence of a hydrophobic pocket of similar volume in all of them, providing enough space to hold a ligand with similar size and properties as the ligand of Pru p 3, hereinafter referred to as CPT-PHS ligand (Fig. 1C).

3.2. The isolated ligands from allergenic LTPs share the same chemical nature

To identify the chemical nature of the natural ligands transported by the selected LTPs, they were purified from different natural sources as previously described [9] and their presence was confirmed by TLC and vanillin staining. All samples showed a single band with a retention factor of 0.5, except Tri a 14, for which at least three different compounds were observed (Fig. 2A). The characterization of the ligands was based on the analysis performed by Cubells-Baeza et al. [9]. All of them showed the same retention time by reversed-phase high-performance liquid chromatography, a single overlapping peak with a retention time of 12 min. However, in the Tri a 14 ligand sample, three different peaks could be noted, in accordance with the observation of the TLC (Fig. 2B).

CPT-PHS ligand was previously identified by mass spectrometry analysis and activity assays were performed to ensure the chemical nature. Camptothecin is able to emit blue autofluorescence under 360 nm and also inhibit topoisomerase I [42] [43]. All the analysed ligands showed the capacity to emit under UV light (Fig. 2C) and inhibit the topoisomerase I activity (Fig. 2D), implying the presence of camptothecin polar head.

On the other hand, previous reports showed that CPT-PHS ligand can stimulate the NF-kB/AP-1 pathway and this activation is due to the presence of a PHS-like fraction in the lipid-ligand and not to the camptothecin polar head [4]. For that reason, the immunological activity was tested in all the purified ligands using THP1-XBlue™ cells, and all of them were able to induce its activation. This result suggests the presence of a fraction in the ligand with the ability to induce the response of the immune system, which could be related to the

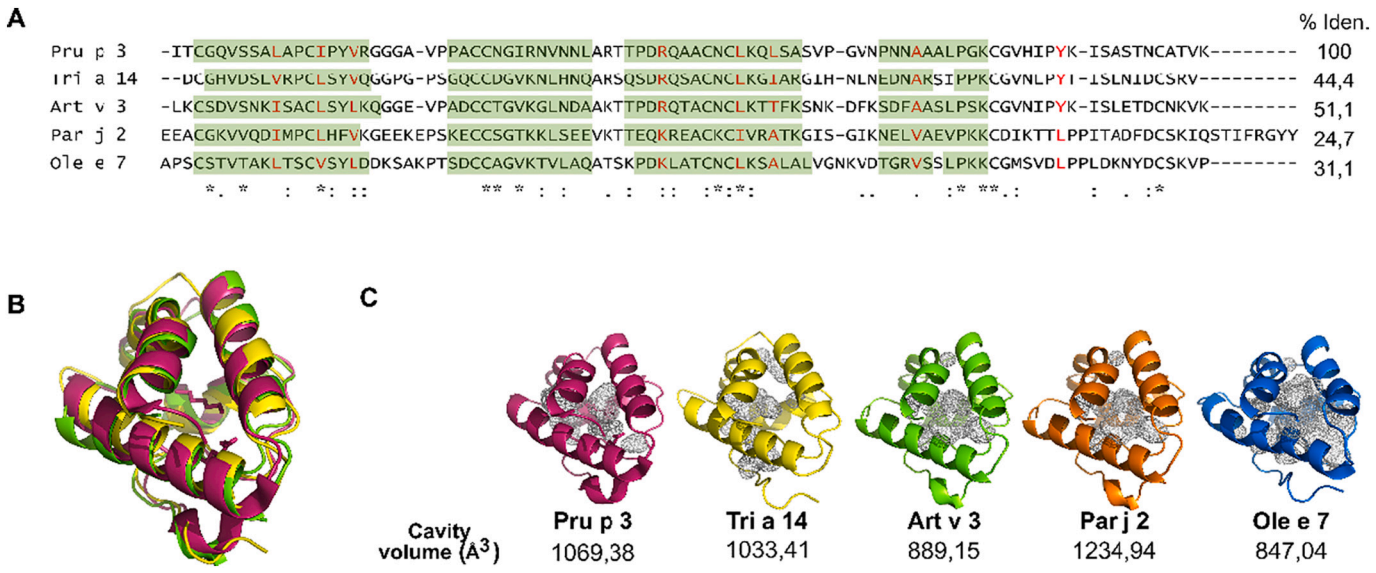

Fig. 1. Characterization of LTPs. **A**) Multiple sequence alignment using Clustal Omega tool. Residues implicated in ligand binding are marked in red. "*" indicates positions which have a single, fully conserved residue; "." indicates conservation between groups of weakly similar properties; ":" indicates conservation between groups of strongly similar properties. Regions predicted to contain an alpha helix secondary structure are shown in green. The % of sequence identity compared to Pru p 3 was calculated for all the LTPs. **B)** Structural alignment using Chimera Software. Pru p 3 (pink) and Tri a 14 (yellow) are experimental structures (PDB entries 2B5S and 1BWO, respectively). Art v 3 (green), Par j 2 (orange) and Ole e 7 (blue) are homology-modelled structures obtained with SwissModel. c) Internal cavity volume of the LTPs (Å^3) calculated with the DogSite method implemented in the Proteins Plus server.

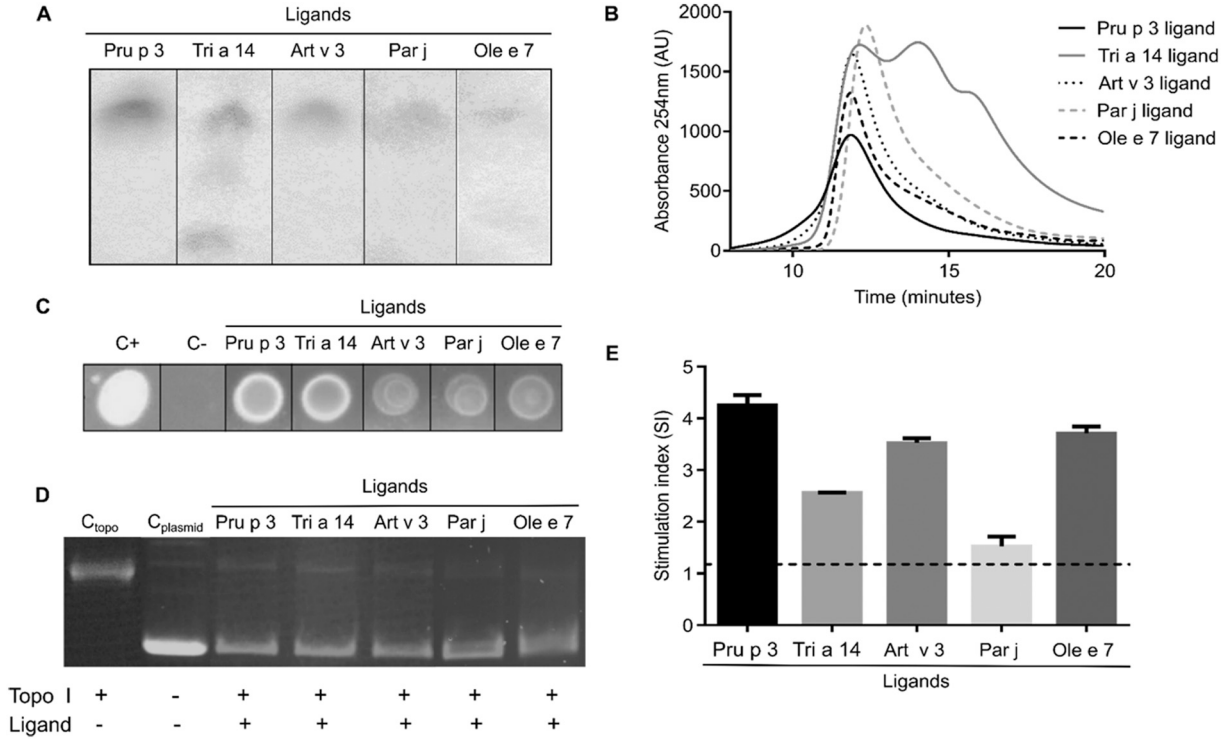

Fig. 2. Characterization of LTP ligands. **A**) Detection of the ligands by TLC in a silica gel plate and stained with vanillin. **B)** Ligand fractionation by phase reverse-HPLC in an isocratic method of 85% acetonitrile and detected at 254 nm. **C)** Emission of the ligands loaded onto a silica gel plate under UV light (365 nm). Commercial OH-CPT was used as positive control. **D)** Inhibition of topoisomerase I activity. Plasmid pGEM was incubated with topoisomerase I in the presence of the ligands and visualized in agarose gel stained with ethidium bromide. **E)** NF-κB/AP-1 activation assay using the transfected cell line THP1-XBlue™. Cells were incubated with each ligand in triplicates and the activation was measured using QUANTI-Blue™. Results were represented by the stimulation index, referenced to the negative control (PBS). The threshold was established as the negative control +3SD.

phytosphingosine tail.

Ligands were finally analysed based on the ESI-QQQ-MS fragmentation pattern of PHS, OH-CPT and the ligand of Pru p 3 previously described. (Fig. 3A, B) [9]. In all cases, it was possible to identify the presence of some characteristic *m/z* peaks from the fragmentation of PHS (m/z values = 115.1; 233.1); OH-CPT (m/z values = 277.1; 321.2;

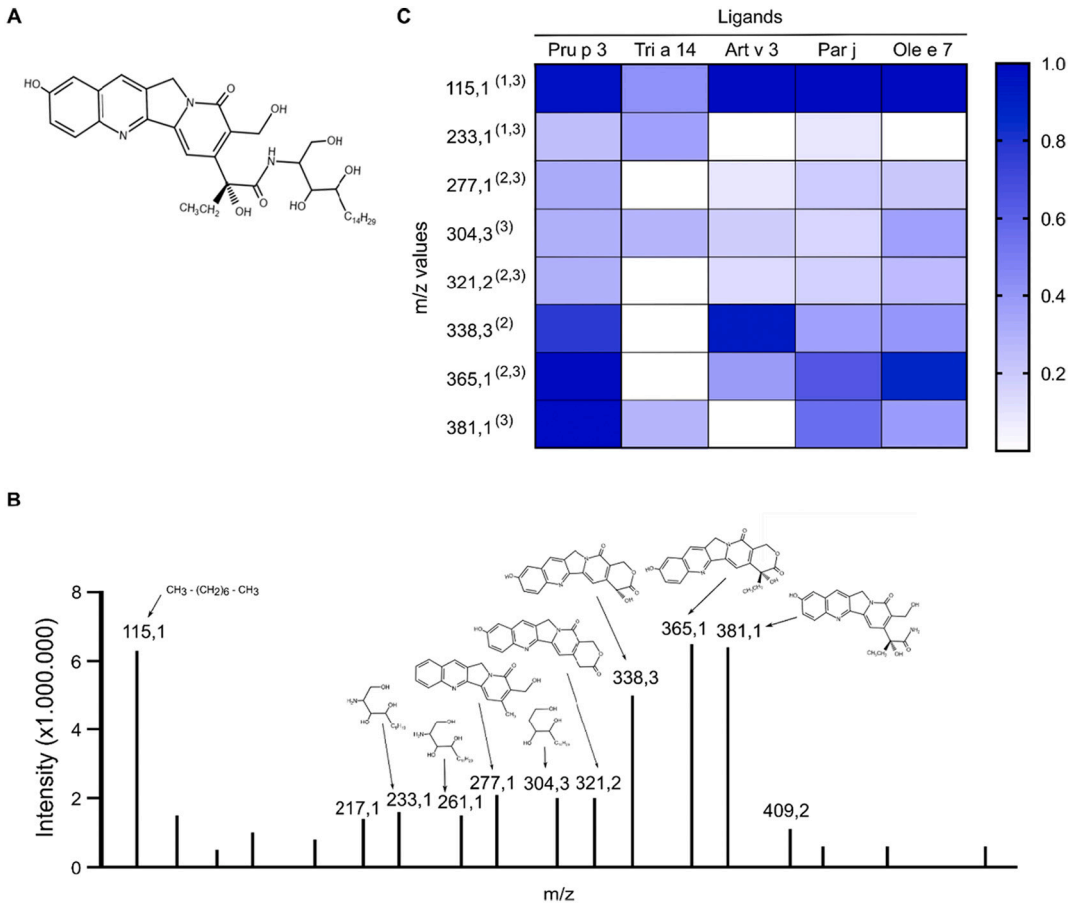

Fig. 3. Identification of the LTP ligands by mass spectrometry (LC-ESI-QQQ) **A)** Structural formula of the ligand of CPT-PHS ligand reported in Cubells-Baeza et al. [9]. **B)** Identification of the m/z values obtained from the fragmentation of the CPT-PHS ligand. Positive ion mass spectra. **C)** Comparison of m/z and relative intensity values obtained for the LTP ligands by mass spectrometry. (1) m/z values coincident with commercial PHS fragmentation; (2) m/z values coincident with commercial OH-CPT fragmentation; (3) m/z values identified as a fragment of the published structure of the CPT-PHS ligand [9].

365.1); and others specific of the link between OH-CPT and PHS moieties (m/z = 304.3; 381.1) (Fig. 3C). The exception was the ligand of Tri a 14 for which the results obtained suggest the presence of a non-hydroxylated CPT. All these data together show that the ligands analysed share a common chemical nature between them and with the one previously described in Cubells-Baeza et al.[9].

In order to carry out the characterization of the binding mode and biological activity, the CPT-PHS ligand was chemically synthesized (sCPT-PHS Ligand).

When the characteristics of the sCPT-PHS ligand were compared with the natural one, similar results were obtained for both of them. The retention time in an isocratic method in the HPLC revealed that both molecules have a similar chemical features (Fig. 4A). Furthermore, both ligands emit under UV light, which may be caused by the presence of a camptothecin-like polar head (Fig. 4B), and both activate the NF-kB pathway, which probably indicates the presence of the phytosphingosine fraction (Fig. 4C). Finally, the stability of the complex formed by Pru p 3 and the sCPT-PHS ligand is comparable with the one formed by the natural one (Fig. 4C), and this stabilization is not due to the separated fractions of the sCPT-PHS ligand (PHS or CPT), as it is later shown in Fig. 5B.

3.3. Binding mode and interaction analysis of Pru p 3

To study the affinity of Pru p 3 to its CPT-PHS ligand and different hydrophobic tails (PHS, stearic acid, oleic acid, and linoleic acid), hydrophobic ELISA plates were used. The Kd values obtained were in the micromolar range for all the lipids. The Kd value for the Pru p 3 and CPT-PHS ligand complex was 0.36 μM while the Kd values for fatty acids were between 0.38 μM for oleic acid to 0.88 μM for linoleic acid. Of note, the PHS alone showed the lowest affinity, with a Kd value of 5.94 μM (Fig. 5A). To confirm these results, an analysis was performed using nanoDSF (Fig. 5B). As it can be seen, Pru p 3 mixed with PHS presented the lowest Tm of all the hydrophobic tails used as well. However, in the case of the CPT-PHS ligand, where PHS is linked to the OH-CPT, the Tm drastically increased. These results highlight the relevance of the polar head in the binding mode.

Finally, computational simulations were used to calculate the energy necessary to tear the lipids from the tunnel of Pru p 3 once they are inside (Fig. 5C). The results are represented in relative terms compared to the molecule on which more energy needs to be applied. As can be observed, once the lipids have been able to bind to Pru p 3, it is necessary to apply more energy to extract CPT-PHS ligand than the rest of the hydrophobic tails, which show no significant differences between them (Fig. 5D). Thus, all these results together seem to indicate that the presence of the polar head plays a role in the interaction with the ligands transported by LTPs.

3.4. Pru p 3 can only bind ligands with a polar head group in a membrane model

In order to verify the role of the polar head in the binding mechanism, the interaction of Pru p 3 with the ligands was studied in a hydrophobic environment using a membrane model based on liposomes of PC. PC was mixed with hydrophobic tails such as PHS, stearic, oleic, and linoleic acid, attached or not to the polar head (alexa fluorescent

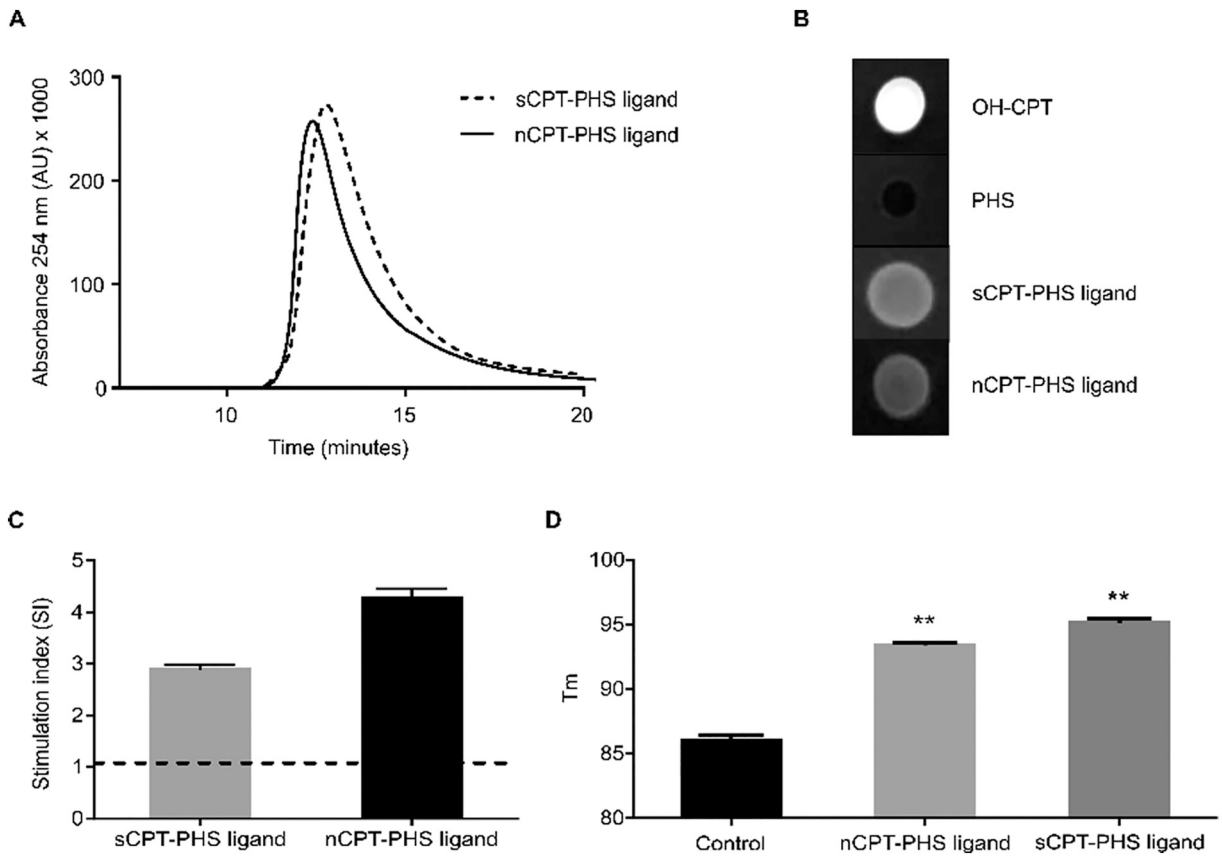

Fig. 4. Characterization of synthetic CPT-PHS ligand. **A)** Elution profiles of sCPT-PHS ligand and nCTP-PHS ligand by phase reverse-HPLC in an isocratic method of 85% acetonitrile and detected at 254 nm. **B)** Emission of sCPT-PHS ligand and native CPT-PHS ligand (nCPT-PHS ligand) loaded onto a silica gel plate under UV light (365 nm). Commercial OH-CPT and PHS were used as controls. **C)** NF-κB/AP-1 activation assay using the transfected cell line THP1-XBlue™. Cells were incubated with each ligand in triplicates and the activation was measured using QUANTI-Blue™. Results were represented by the stimulation index, referenced to the negative control (PBS). The mean of three independent measurements and their SEM is depicted. The threshold was established as the negative control +3SD. **D)** Unfolding transition temperatures (Tm) were calculated by nanoDSF through the incubation of Pru p 3 with sCPT-PHS ligand or nCPT-PHS ligand. The mean Tm of three independent measurements and their SEM is depicted. Pru p 3 without ligand was used as control. **p-value <0.01.

molecule) to form the liposomes.

Liposomes were incubated with labelled rPru p 3 and flow cytometry analysis revealed that Pru p 3 was weakly bound to PC or PC + PHS liposomes. However, when PHS was bound to a polar head as Alexa 488 fluorophore (PC + PHS*), the binding of Pru p 3 drastically increased (Fig. 6A). The proper formation of vesicles and the co-localization of Pru p 3 and labelled PHS was also verified by confocal microscopy (Fig. 6B). The same results were obtained with stearic, oleic, and linoleic acid: Pru p 3 was only able to bind liposomes with these fatty acids when they were labelled with the fluorophore (data not shown).

Same way, when PC liposomes with CPT-PHS ligand were incubated with Pru p 3, binding increase could be observed in comparison to liposomes without ligand (Fig. 6C), with a similar binding percentage than that obtained in the case of liposomes containing labelled PHS.

3.5. *PHS from the CPT-PHS ligand could be phosphorylated by SphK1 in keratinocytes*

To study the role of Pru p 3 bound to CPT-PHS ligand in human epithelia, a skin cellular model based on A431 cells (human epidermal keratinocytes) was developed. Firstly, a keratinocytes monolayer was grown on coverslips, which was then incubated with Pru p 3 complexed with CPT-PHS ligand (complex), CPT-PHS ligand alone, PHS or OH-CPT (Fig. 7A). In the presence of complex, or CPT-PHS ligand after 48 h, cell density was decreased due to cell death as it happened with the incubation of OH-CPT alone. This phenomenon could be due to the ligand cleavage inside the cells, releasing out the polar head, OH-CPT, which has been described as a cytotoxic drug in previous reports [44].

To confirm the fact that the CPT-PHS ligand could be processed by human keratinocytes, a skin cellular model was developed in Transwell® culture plates in the presence of complex, and metabolites in the basolateral media were analysed by ESI-QQQ-MS. The protein fraction (Pru p 3) was not found in the basolateral side (data not shown), suggesting that it was not transported. This is consistent with the role of the skin as a watertight barrier against external agents. In contrast, mass spectrometry revealed the presence of several peaks corresponding to the fragmentation of PHS1P (m/z = 158.00, 166.05, 167.00, and 201.05) (Fig. 7B). Given the fact that PHS is chemically related to sphingosine (SPH), it is likely that it could also be modified by SphK1. This enzyme has been described to phosphorylate SPH into S1P, both in humans and mice [45,46] (Fig. 7C). In the same way, gene expression of the enzyme was increased 10-fold in A431 cells after incubation with the complex, comparing to untreated cells (Fig. 7D). Besides that, complex molecules and SphK1 showed co-localization by immunofluorescence (Fig. 7E).

In order to confirm that the enzyme could also use PHS as substrate, an *in vitro* phosphorylation assay was performed using isolated human enzyme SphK1. A peak corresponding to PHS1P (m/z = 398.4) could be detected after phosphorylation reaction, when products were analysed by MALDI-TOF (Fig. 7F). Furthermore, it was demonstrated that PHS1P is biologically active as it showed chemoattractant activity in a migration assay with the monocytic cell line THP-1 (Fig. 7G).

All these results together confirm that the PHS fraction from CPT-PHS ligand can be modified by human enzymes to produce PHS1P, a

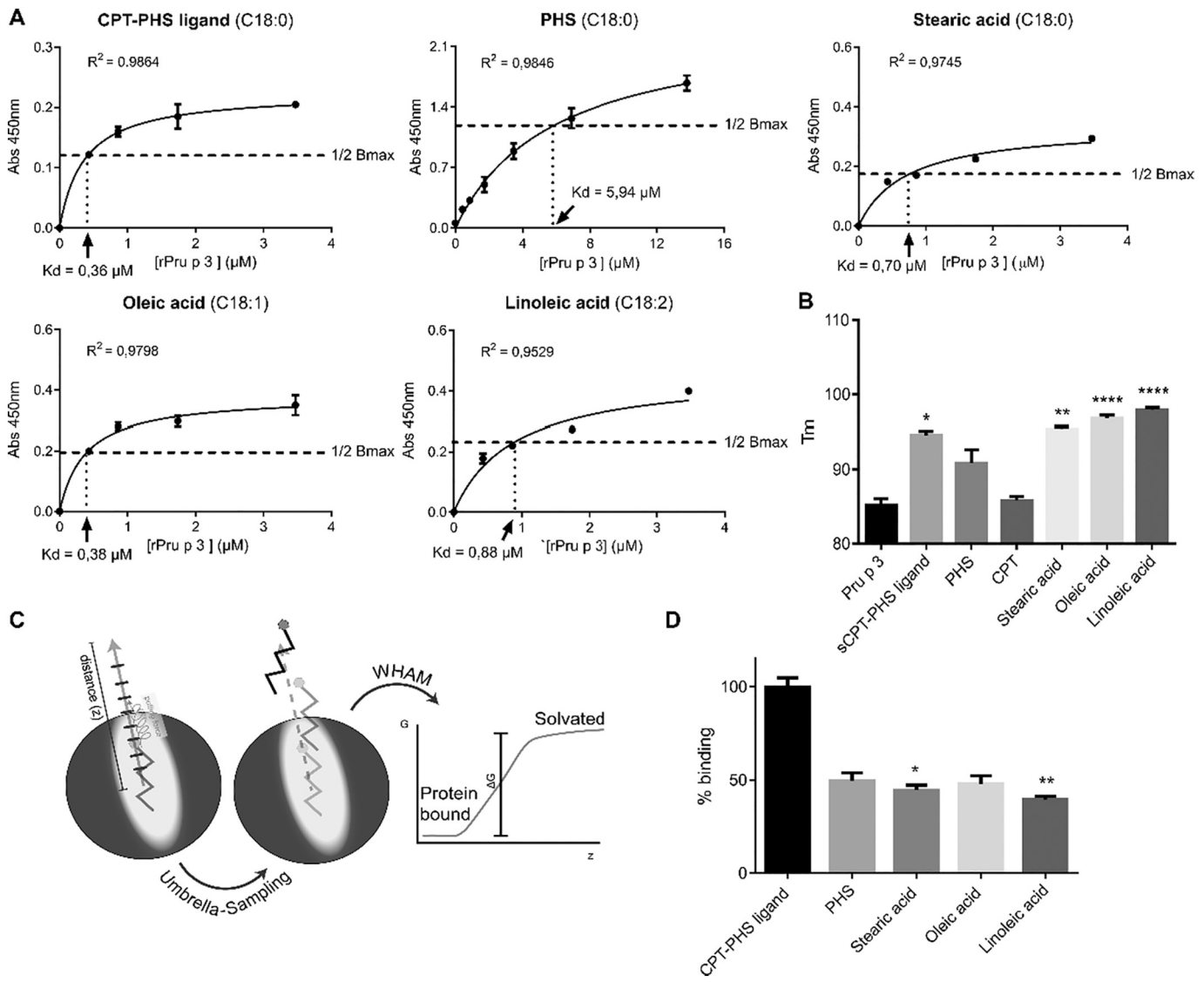

Fig. 5. Binding mode between lipids and Pru p 3. **A)** Increasing concentrations of Pru p 3 were incubated in a 96-well hydrophobic ELISA plate coated with the indicated lipids. Protein binding was revealed using specific polyclonal antibodies against Pru p 3. Graphs illustrate the means of the absorbance values at 450 nm ± SEM, $n = 3$. **B)** Unfolding transition temperatures (Tm) were calculated by nanoDSF through the incubation of Pru p 3 with different ligands. The mean Tm of three independent measurements and their SEM is depicted. Pru p 3 without ligand was used as control. **C)** Diagram of the umbrella sampling molecular dynamics (MD) protocol. It consists of the following steps: left) Generate a set of windows using a reaction variable, which in this case is the distance between the centres of mass of the ligand and the protein; centre) simulate the ligand inside each of this windows by constraining its position using a harmonic restraint; right) recover the unperturbed histogram by applying the weighted histogram analysis method (WHAM) on the perturbed trajectory. The result is a curve of mean potential force from which the binding free energy can be derived as the difference between the minimum (protein state) and maximum (solvated state). **D)** Relative energy necessary to apply to different ligands for pulling out the from Pru p 3 with regard to CPT-PHS ligand taken as 100% reference. Data obtained from the computational MD simulation. The mean and SEM of five replicates for each ligand are represented. *p-value<0.05, **p-value <0.01, ***p-value <0.001.

molecule that seems to mimic S1P immunological activity.

4. Discussion

LTPs are widely distributed throughout the plant kingdom. They are found in all land plants [47] and they are implicated in relevant processes for plant growth and maturing, such as signaling [48], reproduction [49] or seed and fruit development [50], among others [47]. In humans, they are involved in the development of allergies, being major allergens of different fruits, vegetables and nuts in the Mediterranean area [51]. Nevertheless, it has been demonstrated that not only the proteins themselves are relevant in the development of allergic reactions, but also their ligands, especially during the sensitization phase [4].

Since LTPs have been found to take and transfer lipids, their binding capacity and the molecular features of these ligands have been studied. Due to their large hydrophobic cavity, it has been shown that several LTPs can bind a wide range of ligands *in vitro*, including fatty acids (FAs), acyl derivatives of coenzyme A (CoA), phospho- and galactolipids, prostaglandin B2, molecules of organic solvents, and some drugs [52–56]. However, these ligand-binding studies have not deepened in the understanding of their *in vivo* functions and binding capacity [47].

The first natural ligand of an LTP identified was that of Pru p 3, the major allergen from peach. That ligand was characterized as a derivative of camptothecin (OH-CPT) linked by an amide bond to a PHS tail [9]. Following that line of study, the natural ligands transported by other four allergenic LTPs from *Triticum aestivum, Artemisia vulgaris, Parietaria judaica* and *Olea europea* were analysed and the results showed that the

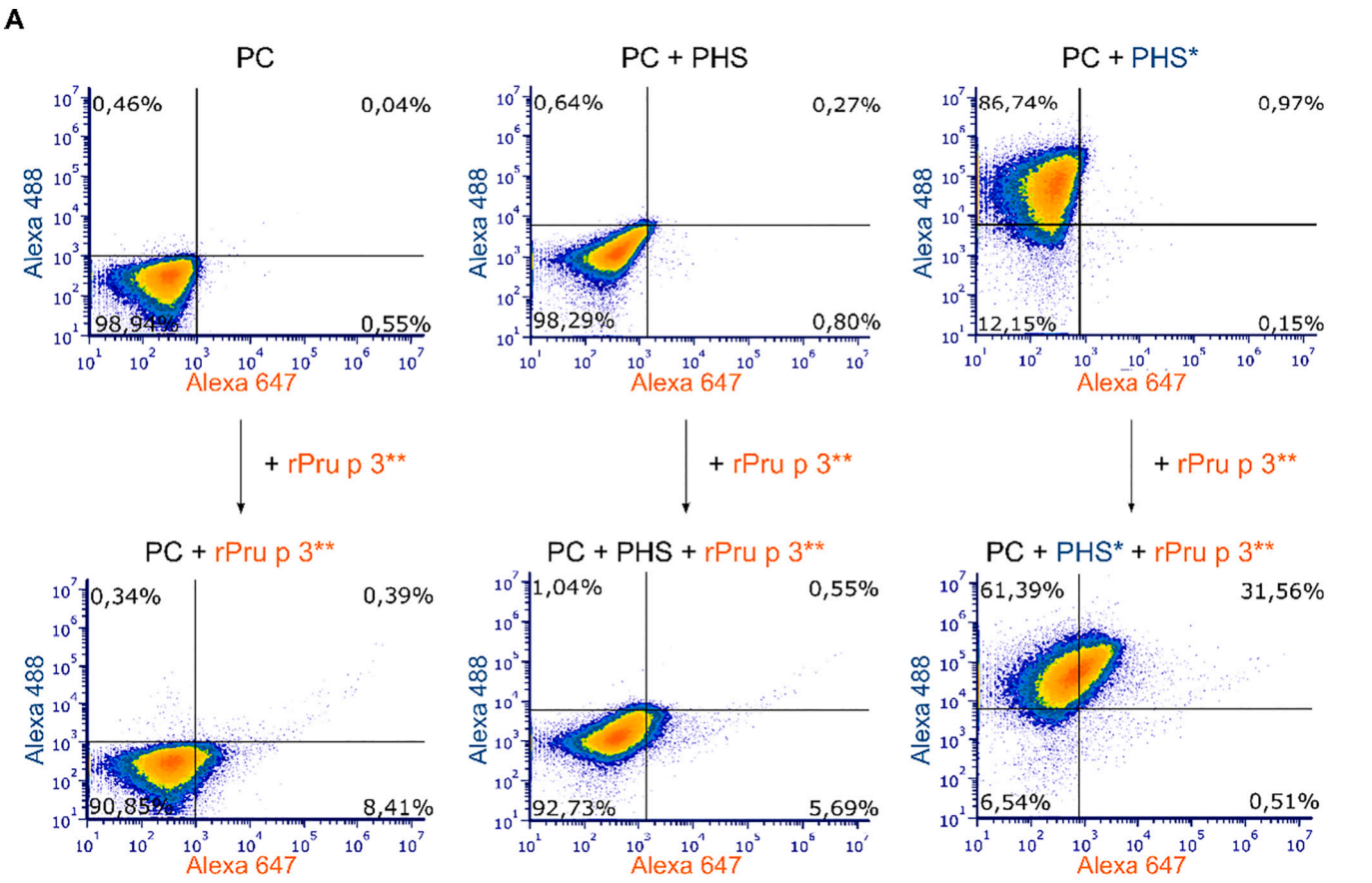

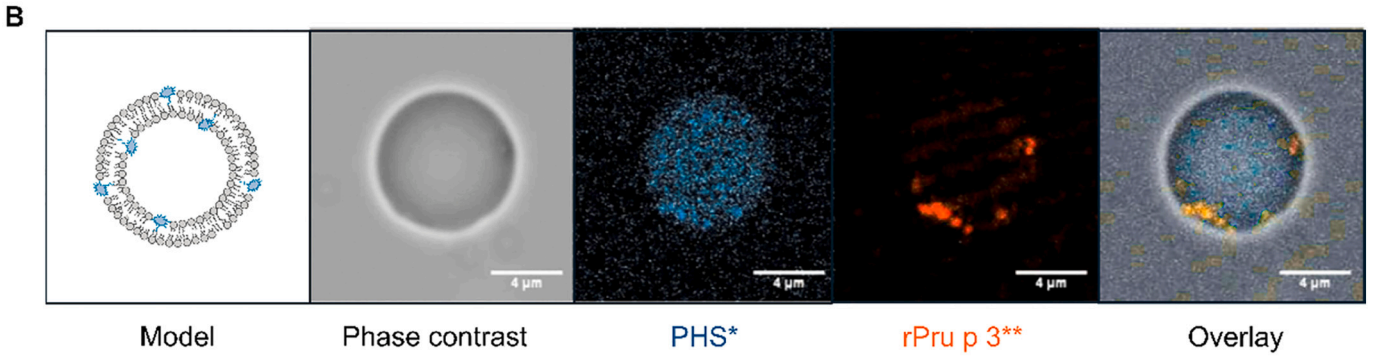

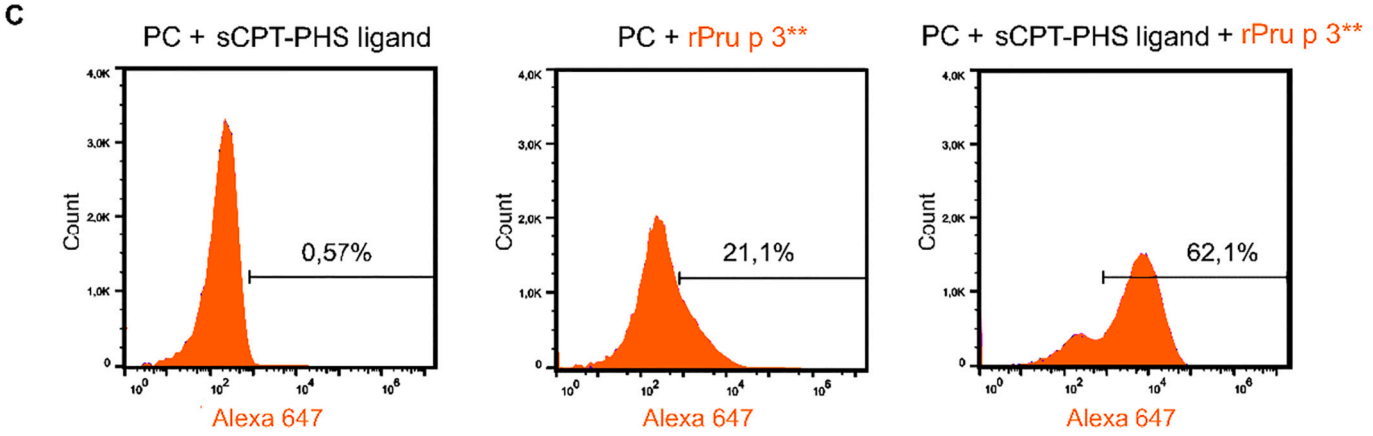

(caption on next page)

Fig. 6. Binding specificity of Pru p 3 in a liposome membrane model. **A)** Liposomes of phosphatidylcholine (PC), PC and phytosphingosine (PC + PHS), and PC and labelled PHS (PC + PHS*) were produced and incubated for 2 h with labelled Pru p 3 (Pru p 3**). The binding was studied by flow cytometry. **B)** Model of liposomes structure is depicted in the figure. Liposomes of PC and PHS* incubated with Pru p 3** (PC + PHS* + Pru p 3**) were visualized by confocal microscopy. **C)** Liposomes of PC and PC + CPT-PHS ligand were incubated with Pru p 3**. The binding was studied by flow cytometry. Representative data are shown from three independent experiments.

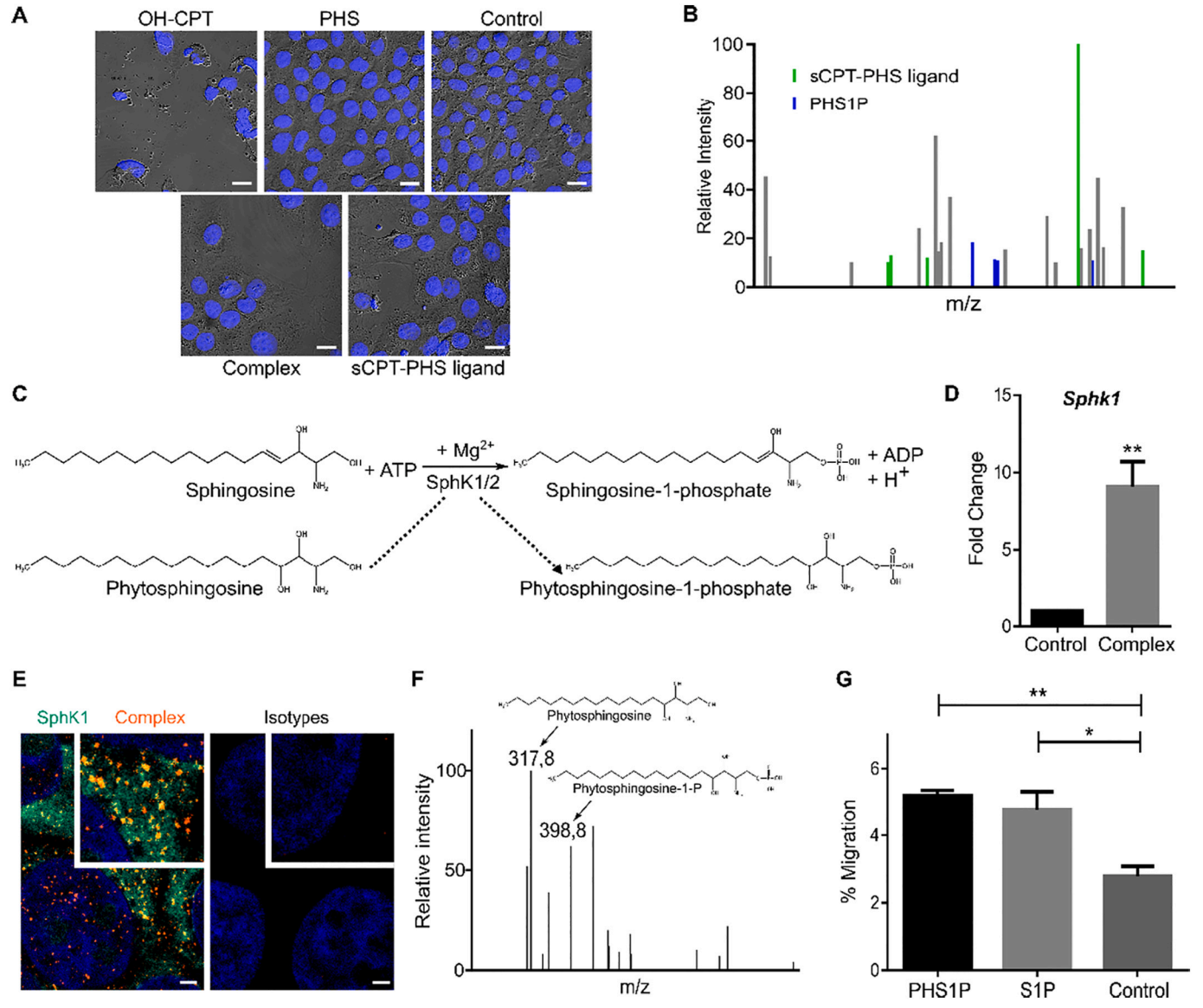

Fig. 7. The CPT-PHS ligands metabolized into a S1P-like molecule. **A)** A431 cells were seeded in coverslips and incubated with complex (Pru p 3 + CPT-PHS ligand (10:1), CPT-PHS ligand, PHS, OH-CPT or PBS for 48 h. Cell density was analysed by confocal microscopy after DAPI staining. Bar = 20 μm. **B)** *In vitro* skin cellular model was incubated with complex or PBS. After five days, basolateral media were analysed by ESI-QQQ-MS and the identification of metabolites was carried using standards as fragmentation control. **C)** Scheme of the phosphorylation reaction catalyzed by SphK1. **D)** A431 cells were incubated with complex for 72 h. Relative expression of *Sphk1* gene was analysed by RTqPCR. Results are shown as Fold Change = 2 · (Ct GAPDH – Ct gene) / 2 · (Ct GAPDH control – Ct gene control). Data obtained from three independent experiments are presented as mean and SEM. **E)** Immunofluorescence of A431 cells incubated with complex (orange) co-locating with SphK1 (green). Nuclei stained with DAPI (blue). Bar = 2 μm. **F)** *In vitro* phosphorylation of the PHS fraction of CPT-PHS ligand by SphK1, analysed by MALDI-TOF. Substrate-free reaction was used as negative control. **G)** THP-1 cells were seeded in 24-well Transwell® culture plates and PHS, PHS1P, S1P or RPMI were added in the basolateral chamber. After 6 h the number of cells in the basolateral side were counted by flow cytometry. The percentage of cell migration of three independent experiment is depicted (mean ± SEM). *p-values <0.05, **p-value<0.01.

carried ligands have the same chemical nature. Moreover, when studying the binding affinity of Pru p 3 *in vitro* for different lipid tails and its CPT-PHS ligand, it was shown that all of them have slightly different Kd values over the micromolar (μM) range, in agreement with results reported by other authors [57] and with the ones obtained by measurement of thermal stability. However, computational methods, which account for the energy necessary to pull out the ligands from the cavity of Pru p 3, suggest that the complex of Pru p 3 and CPT-PHS ligand is more stable than the other ones. Furthermore, when *in vivo* function of LTPs was mimicked by using liposome membrane models, results showed that the presence of a polar head attached to the hydrophobic tail significantly increases the binding of Pru p 3. In combination, these

results show that the presence of the polar head is key in the binding process. Although this is probably not caused by an increase in the binding affinity, it suggests that its presence clearly promotes the anchorage, making its extraction more difficult, which in turn supports the hypothesis that all the LTPs analysed carry indeed the same ligand.

Considering that the polar head in the natural ligands has been identified as a derivative of camptothecin, the set of lipids that it can be attached to is limited. The presence of an amine group in the lipid tail is necessary to form an amide bond with the carboxyl group in the camptothecin moiety. Although that functional group is not present in the fatty acids studied here, it is present in long-chain bases (LCB) like PHS, which are part of the sphingolipids. Sphingolipids are estimated to constitute up to 30% of the tonoplast and plasma membrane lipids in plants [58], and specifically, PHS is the major LCB in plants [59].

Regarding the pathophysiological role of PHS in human allergies, it must be taken into account that molecules with similar structures usually show similar functionalities [60]. Following that principle, PHS could be a functional analogue of human SPH, since these two molecules only differ in the presence of a hydroxyl group. It is known that SPH is converted by the epithelial enzyme SphK1 into S1P, a metabolite with an important role in the pathogenesis of allergy [61]. The results presented here show that PHS can also act as a substrate to this enzyme, which metabolizes it into PHS1P. However, the enzyme was not able to phosphorylate the complete CPT-PHS ligand, which seems to suggest that PHS can only be converted into PHS1P by human epithelia if the amide bond of the ligand is broken. In accordance with that observation, it is here reported that the ligand of Pru p 3 shows pro-apoptotic effects over human keratinocytes, which is a direct effect of its free camptothecin fraction, as OH-CPT has been used as a cytotoxic drug [44]. Since the formation of an amide bond prevents the active form of CPT [9], it is concluded that the CPT-PHS ligand of the LTPs is intracellularly processed into its different components, resulting in the release of free PHS, which is subsequently converted into PHS1P, an analogue of S1P, by SphK1. The fact that human keratinocytes overexpress sphingosine kinase transcripts upon incubation with complex furtherly supports this theory. In fact, the results also show that SphK1 co-locates with Pru p 3, suggesting an interaction between the enzyme and the ligand present inside its cavity.

Finally, the presence of PHS1P in the supernatants of human keratinocytes cultured with Pru p 3 and CPT-PHS ligand complexed might evidence its putative role as a chemical signal used by the epithelium to attract immune cells to the site of inflammation. It is well-known that S1P interaction is needed for the egress of immune cells from lymphoid organs (such as thymus and lymph nodes) into the lymphatic vessels [62]. Concerning other type 2 diseases (such as allergy), S1P has been reported to play an important role in the pathogenesis of asthma and atopic dermatitis [63,64]. Here, it is demonstrated that PHS1P acts as a chemoattractant to human monocytes, with an efficacy comparable to that of S1P. That could explain the immunogenic property exerted by the CPT-PHS ligand in previous reports [4]. Although the results obtained pointed out the phosphorylation as a possible metabolic mechanism, it should be taken into account that the biosynthesis and metabolism of sphingolipids involve more than 40 enzymes in mammals [65]. Therefore, PHS could not only be phosphorylated but also implicated in other metabolic pathways.

In conclusion, natural ligands isolated from four different allergenic LTPs have been characterized and compared with the previously described CPT-PHS ligand of Pru p 3, identifying a chemical nature common to all of them. Despite the ability of LTPs to bind a huge amount of lipids *in vitro*, the presence of a polar head attached to the ligand structure plays a key role in the stabilization of the binding. This fact significantly reduces the number of molecules that *in vivo* can be attached to these proteins, limiting it to molecules with a lipid tail belonging to the sphingolipid family, being PHS the most representative in plants. Once inside the epithelial cells, the associated lipid tail is cleaved and recognized by enzymes involved in its phosphorylation process, leading to the release of PHS1P, a functional analogue of the S1P.

These data together could help to understand why LTPs are associated with more severe allergic responses. To continue this study, it would be interesting to identify the natural ligand of non-allergenic members of the LTP protein family as well as to study the capacity of non-allergenic LTPs to bind the CPT-PHS ligand of allergenic LTPs. That could definitely demonstrate the potential of the ligands transported by LTPs during the sensitization phase of allergic reactions.

Funding

This research was funded by the Spanish Government (MINECO, grant BIO2017-84548- R); Instituto de Salud Carlos III (ISCIII) co-founded by FEDER Thematic Networks and Cooperative Research Centers: ARADYAL (RD16/0006/0003), the Community of Madrid (FOODAL-CM_S2018/BAAA-4574), European Commission (H2020-NMBP-X-KET-2017 - 768641 – AllerScreening) and Universidad Politécnica de Madrid and Banco Santander for a predoctoral Programa Propio grant.

CRediT authorship contribution statement

Zulema Gonzalez-Klein: Formal analysis, Investigation, Methodology, Visualization, Writing – original draft. **Bruno Cuevas-Zuviria:** Investigation, Methodology, Formal analysis, Visualization. **Andrea Wangorsch:** Investigation, Methodology, Formal analysis. **Guadalupe Hernandez-Ramirez:** Investigation, Methodology, Formal analysis. **Diego Pazos-Castro:** Investigation, Methodology, Formal analysis. **Carmen Oeo-Santos**: Investigation, Methodology, Formal analysis. **Alejandro Romero-Sahagun**: Writing-review & editing. **Luis F. Pacios:** Methodology, Validation, Writing – review & editing. **Jaime Tome-Amat:** Investigation, Methodology, Formal analysis. **Stephan Scheurer:** Conceptualization, Resources, Writing – review & editing. **Araceli Diaz-Perales:** Conceptualization, Funding acquisition, Project administration, Validation, Writing – original draft, Resources. **María Garrido-Arandia:** Conceptualization, Project administration, Resources, Supervision, Validation, Visualization, Writing – original draft.

Declaration of competing interest

The authors declare that they have no known competing financial interest or personal relationship that could have appeared to influence the work reported in this paper.

References

[1] A.K. Abbas, A.H. Lichtman, S. Pillai, Cellular and Molecular Immunology, Elsevier Saunders, Philadelphia (USA, 2015.
[2] J.K. Actor, Integrated Immunology and Microbiology, Second, Elsevier Saunders, Philadelphia (USA, 2012.
[3] M. Adriano, R. Chiara, P. Palazzo, E. Scala, Allergen databases: current status and perspectives, Curr, Allergy Asthma Rep. 9 (2009) 376–383, https://doi.org/10.1007/s11882-009-0055-9.
[4] L. Tordesillas, N. Cubells-Baeza, C. Gómez-Casado, C. Berin, V. Esteban, W. Barcik, L. O'Mahony, C. Ramirez, L.F. Pacios, M. Garrido-Arandia, A. Díaz-Perales, Mechanisms underlying induction of allergic sensitization by Pru p 3, Clin, Exp. Allergy. 47 (2017) 1398–1408, https://doi.org/10.1111/cea.12962.
[5] M. Ebisawa, B.K. Ballmer-Weber, S. Vieths, R.A. Wood, Food Allergy: Molecular Basis and Clinical Practice, S, Karger AG, Freiburg im Breisgau, 2015, https://doi.org/10.2340/00015555-2256.
[6] M. Bublin, T. Eiwegger, H. Breiteneder, Do lipids influence the allergic sensitization process? J. Allergy Clin. Immunol. 134 (2014) 521–529, https://doi.org/10.1016/j.jaci.2014.04.015.
[7] T. Jacob, C.S. von Loetzen, A. Reuter, U. Lacher, D. Schiller, R. Schobert, V. Mahler, S. Vieths, P. Rösch, K. Schweimer, B.M. Wöhrl, Identification of a natural ligand of the hazel allergen Cor a 1, Sci, Rep. 9 (2019), https://doi.org/10.1038/s41598-019-44999-2.
[8] C.S. Von Loetzen, T. Hoffmann, M.J. Hartl, K. Schweimer, W. Schwab, P. Rösch, O. Hartl-Spiegelhauer, Secret of the major birch pollen allergen Bet v 1: identification of the physiological ligand, Biochem. J. 457 (2014) 379–390, https://doi.org/10.1042/BJ20130413.

[9] N. Cubells-Baeza, C. Gómez-Casado, L. Tordesillas, C. Ramírez-Castillejo, M. Garrido-Arandia, P. González-Melendi, M. Herrero, L.F. Pacios, A. Díaz-Perales, Identification of the ligand of Pru p 3, a peach LTP, Plant Mol, Biol. 94 (2017) 33–44, https://doi.org/10.1007/s11103-017-0590-z.
[10] R.J. Dearman, M.J.C. Alcocer, I. Kimber, Influence of plant lipids on immune responses in mice to the major Brazil nut allergen Ber e 1, Clin, Exp. Allergy. 37 (2007) 582–591, https://doi.org/10.1111/j.1365-2222.2007.02689.x.
[11] A. Angelina, S. Sirvent, C. Palladino, A. Vereda, J. Cuesta-Herranz, T. Eiwegger, R. Rodríguez, H. Breiteneder, M. Villalba, O. Palomares, The lipid interaction capacity of Sin a 2 and Ara h 1, major mustard and peanut allergens of the cupin superfamily, endorses allergenicity, Allergy. 71 (2016) 1284–1294, https://doi.org/10.1111/all.12887.
[12] K. Hufnagl, D. Ghosh, S. Wagner, A. Fiocchi, L. Dahdah, R. Bianchini, N. Braun, R. Steinborn, M. Hofer, M. Blaschitz, G.A. Roth, G. Hofstetter, F. Roth-Walter, L. F. Pacios, E. Jensen-Jarolim, Retinoic acid prevents immunogenicity of milk lipocalin Bos d 5 through binding to its immunodominant T-cell epitope, Sci, Rep. 8 (2018) 1598, https://doi.org/10.1038/s41598-018-19883-0.
[13] M. Basagaña Torrentó, C. Elduque, A. Teniente-Serra, I. Casas, A. Roger, Clinical profile of lipid transfer protein syndrome in a mediterranean area, J Investig Allergol Clin Immunol 28 (2018) 58–60, https://doi.org/10.18176/jiaci.0209.
[14] G. Salcedo, R. Sánchez-Monge, D. Barber, A. Díaz-Perales, Plant non-specific lipid transfer proteins: An interface between plant defence and human allergy, Biochim, Biophys. Acta - Mol. Cell Biol. Lipids. 1771 (2007) 781–791, https://doi.org/10.1016/j.bbalip.2007.01.001.
[15] L.F. Pacios, C. Gómez-Casado, L. Tordesillas, A. Palacín, R. Sánchez-Monge, A. Díaz-Perales, Computational study of ligand binding in lipid transfer proteins: structures, interfaces, and free energies of protein-lipid complexes, J. Comput. Chem. 33 (2012) 1831–1844, https://doi.org/10.1002/jcc.23012.
[16] L. Tordesillas, L.F. Pacios, A. Palacin, S. Quirce, A. Armentia, D. Barber, G. Salcedo, A. Diaz-Perales, Molecular basis of allergen cross-reactivity: non-specific lipid transfer proteins from wheat flour and peach fruit as models, Mol, Immunol. 47 (2009) 534–540, https://doi.org/10.1016/j.molimm.2009.07.028.
[17] A. Wangorsch, S. Schülke, G. Gadermaier, M. Albrecht, M. Wallner, S. Randow, S. Wolfheimer, J. Lidholm, I. Lauer, F. Ferreira, M. Toda, S. Vieths, G. Reese, S. Scheurer, LTP cross-reactivity - primary sensitization to mugwort pollen LTP Art v 3, facilitates subsequent sensitisation to peach LTP Pru p 3 in mice, Clin, Transl. Allergy. 4 (2014), O14, https://doi.org/10.1186/2045-7022-4-s2-o14.
[18] P. Dubiela, R. Del Conte, F. Cantini, T. Borowski, R. Aina, C. Radauer, M. Bublin, K. Hoffmann-Sommergruber, S. Alessandri, Impact of lipid binding on the tertiary structure and allergenic potential of Jug r 3, the non-specific lipid transfer protein from walnut, Sci, Rep. 9 (2019) 1–11, https://doi.org/10.1038/s41598-019-38563-1.
[19] R. Apweiler, A. Bairoch, C.H. Wu, W.C. Barker, B. Boeckmann, S. Ferro, E. Gasteiger, H. Huang, R. Lopez, M. Magrane, M.J. Martin, D.A. Natale, C. O'Donovan, N. Redaschi, L.L. Yeh, UniProt: the universal protein knowledgebase, Nucleic Acids Res. 32 (2004) 115–119, https://doi.org/10.1093/nar/gkh131.
[20] F. Sievers, A. Wilm, D. Dineen, T.J. Gibson, K. Karplus, W. Li, R. Lopez, H. McWilliam, M. Remmert, J. Söding, J.D. Thompson, D.G. Higgins, Fast, scalable generation of high-quality protein multiple sequence alignments using Clustal omega, Mol, Syst. Biol. 7 (2011), https://doi.org/10.1038/msb.2011.75.
[21] D.T. Buchan, W.A. Jones Daniel, The PSIPRED protein analysis workbench: 20 years on, Nucleic Acids Res. 47 (2019) 402–407, https://doi.org/10.1093/nar/gkz297.
[22] N. Pasquato, R. Berni, C. Folli, S. Folloni, M. Cianci, S. Pantano, J.R. Helliwell, G. Zanotti, Crystal structure of peach Pru p 3, the prototypic member of the family of plant non-specific lipid transfer protein pan-allergens, J. Mol. Biol. 356 (2006) 684–694, https://doi.org/10.1016/j.jmb.2005.11.063.
[23] D. Charvolin, J.P. Douliez, D. Marion, C. Cohen-Addad, E. Pebay-Peyroula, The crystal structure of a wheat nonspecific lipid transfer protein (ns- LTP1) complexed with two molecules of phospholipid at 2.1 Å resolution, Eur. J. Biochem. 264 (1999) 562–568, https://doi.org/10.1046/j.1432-1327.1999.00667.x.
[24] M. Biasini, S. Bienert, A. Waterhouse, K. Arnold, G. Studer, T. Schmidt, F. Kiefer, T. G. Cassarino, M. Bertoni, L. Bordoli, T. Schwede, SWISS-MODEL: modelling protein tertiary and quaternary structure using evolutionary information, Nucleic Acids Res. 42 (2014), https://doi.org/10.1093/nar/gku340.
[25] K. Arnold, L. Bordoli, J. Kopp, T. Schwede, The SWISS-MODEL workspace: a web-based environment for protein structure homology modelling, Bioinformatics. 22 (2006) 195–201, https://doi.org/10.1093/bioinformatics/bti770.
[26] E.F. Pettersen, T.D. Goddard, C.C. Huang, G.S. Couch, D.M. Greenblatt, E.C. Meng, T.E. Ferrin, U.C.S.F. Chimera, A visualization system for exploratory research and analysis, J. Comput. Chem. 25 (2004) 1605–1612, https://doi.org/10.1002/jcc.20084.
[27] A. Volkamer, D. Kuhn, F. Rippmann, M. Rarey, Dogsitescorer: a web server for automatic binding site prediction, analysis and druggability assessment, Bioinformatics. 28 (2012) 2074–2075, https://doi.org/10.1093/bioinformatics/bts310.
[28] A. Diaz Perales, G. Garcia Casado, R. Sanchez Monge, F.J. Garcia Selles, D. Barber, G. Salcedo, cDNA cloning and heterologous expression of the major allergens from peach and apple belonging to the lipid-transfer protein family, Clin, Exp. Allergy. 32 (2002) 87–92, https://doi.org/10.1046/j.0022-0477.2001.01257.x.
[29] A. Akbarzadeh, R. Rezaei-Sadabady, S. Davaran, S.W. Joo, N. Zarghami, Y. Hanifehpour, M. Samiei, M. Kouhi, K. Nejati-Koshki, Liposome: classification, preparation, and applications, Nanoscale Res. Lett. 8 (2013) 1–9, https://doi.org/10.1186/1556-276X-8-102.
[30] S. Abd-Elhadi, M. Basora, D. Vilas, E. Tolosa, R. Sharon, Total α-synuclein levels in human blood cells, CSF, and saliva determined by a lipid-ELISA, Anal, Bioanal. Chem. 408 (2016) 7669–7677, https://doi.org/10.1007/s00216-016-9863-7.
[31] J. Kästner, Umbrella sampling, WIREs Comput, Mol. Sci. 1 (2011) 932–942, https://doi.org/10.1002/wcms.66.
[32] O. Trott, A.J. Olson, AutoDock Vina: improving the speed and accuracy of docking with a new scoring function, efficient optimization, and multithreading, J. Comput. Chem. 31 (2009) NA-NA. doi:https://doi.org/10.1002/jcc.21334.
[33] S. Jo, X. Cheng, J. Lee, S. Kim, S.-J. Park, D.S. Patel, A.H. Beaven, K. Il Lee, H. Rui, S. Park, H.S. Lee, B. Roux, A.D. MacKerell, J.B. Klauda, Y. Qi, W. Im, CHARMM-GUI 10 years for biomolecular modeling and simulation, J. Comput. Chem. 38 (2017) 1114–1124, https://doi.org/10.1002/jcc.24660.
[34] K. Vanommeslaeghe, E. Hatcher, C. Acharya, S. Kundu, S. Zhong, J. Shim, E. Darian, O. Guvench, P. Lopes, I. Vorobyov, A.D. Mackerell, CHARMM general force field: a force field for drug-like molecules compatible with the CHARMM all-atom additive biological force fields, J. Comput. Chem. 31 (2010) 671–690, https://doi.org/10.1002/jcc.21367.
[35] J.C. Phillips, R. Braun, W. Wang, J. Gumbart, E. Tajkhorshid, E. Villa, C. Chipot, R. D. Skeel, L. Kalé, K. Schulten, Scalable molecular dynamics with NAMD, J. Comput. Chem. 26 (2005) 1781–1802, https://doi.org/10.1002/jcc.20289.
[36] G. Fiorin, M.L. Klein, J. Hénin, Using collective variables to drive molecular dynamics simulations, Mol, Phys. 111 (2013) 3345–3362, https://doi.org/10.1080/00268976.2013.813594.
[37] S. Kumar, J.M. Rosenberg, D. Bouzida, R.H. Swendsen, P.A. Kollman, Multidimensional free-energy calculations using the weighted histogram analysis method, J. Comput. Chem. 16 (1995) 1339–1350, https://doi.org/10.1002/jcc.540161104.
[38] A. Grossfield, WHAM: an implementation of the weighted histogram analy-sis method, (n.d.).
[39] Y. Konishi, K. Hagiwara, M. Shimizu, Transepithelial transport of fluorescein in Caco-2 cell monolayers and use of such transport in in vitro evaluation of phenolic acid availability, Biosci. Biotechnol. Biochem. 66 (2002) 2449–57. doi:https://doi.org/10.1271/bbb.66.2449.
[40] S.C. Sapcariu, T. Kanashova, D. Weindl, J. Ghelfi, G. Dittmar, K. Hiller, Simultaneous extraction of proteins and metabolites from cells in culture, MethodsX. 1 (2014) 74–80, https://doi.org/10.1016/j.mex.2014.07.002.
[41] C.R. Justus, N. Leffler, M. Ruiz-Echevarria, L.V. Yang, In vitro cell migration and invasion assays, J. Vis. Exp. 88 (2014), https://doi.org/10.3791/51046.
[42] C.M. Wright, A.H. van der Merwe, Marié DeBrot, M.-A. Bjornsti, DNA topoisomerase I domain interactions impact enzyme activity and sensitivity to camptothecin, J. Biol. Chem. 290 (2015) 12068–78. doi:https://doi.org/10.1074/jbc.M114.635078.
[43] S. Sirikantaramas, H. Sudo, T. Asano, M. Yamazaki, K. Saito, Transport of camptothecin in hairy roots of Ophiorrhiza pumila, Phytochemistry. 68 (2007) 2881–2886, https://doi.org/10.1016/j.phytochem.2007.08.028.
[44] Z. Ruiwen, L. Yufeng, C. Qiuyin, S. Tiepu Liu He, B. Chambless, Preclinical pharmacology of the natural product anticancer agent 10-hydroxycamptothecin, an inhibitor of topoisomerase I, Cancer Chemother. Pharmacol. 41 (1998) 257–267, https://doi.org/10.1007/s002800050738.
[45] S. Pyne, N. Pyne, Sphingosine 1-phosphate signalling in mammalian cells, Biochem. J. 349 (2000) 385–402, https://doi.org/10.1042/0264-6021:3490385.
[46] Z. Wang, X. Min, S.-H. Xiao, D. Johnstone, Sheree Romanow, William Meininger, H. Xu, J. Liu, J. Dai, S. An, S. Thibault, N. Walker, Molecular basis of sphingosine kinase 1 substrate recognition and catalysis, Structure. 21 (2013) 798–809, https://doi.org/10.1016/j.str.2013.02.025.
[47] T.A. Salminen, K. Blomqvist, J. Edqvist, Lipid transfer proteins: classification, nomenclature, structure, and function, Planta. 244 (2016) 971–997, https://doi.org/10.1007/s00425-016-2585-4.
[48] A.M. Maldonado, P. Doerner, R.A. Dixon, C.J. Lamb, R.K. Cameron, A putative lipid transfer protein involved in systemic resistance signalling in Arabidopsis, Nature. 419 (2002) 399–403, https://doi.org/10.1038/nature00962.
[49] S. Park, G. Jauh, J. Mollet, K.J. Eckard, E.A. Nothnagel, L.L. Walling, E.M. Lord, A lipid transfer – like protein is necessary for lily pollen tube adhesion to an in vitro stylar matrix, Plant Cell 12 (2000) 151–163, https://doi.org/10.1105/tpc.12.1.151.
[50] J. Royo, E. Gómez, O. Sellam, D. Gerentes, W. Paul, G. Hueros, Transcribed in a non-overlapping spatial pattern on the outer surface of the developing endosperm 5 (2014) 1–11, https://doi.org/10.3389/fpls.2014.00180.
[51] M. Egger, M. Hauser, A. Mari, F. Ferreira, G. Gadermaier, A. Mari, The role of lipid transfer proteins in allergic diseases, Curr, Allergy Asthma Rep. 10 (2010) 326–335, https://doi.org/10.1007/s11882-010-0128-9.
[52] E.I. Finkina, D.N. Melnikova, I. V. Bogdanov, T. V. Ovchinnikova, Lipid transfer proteins as components of the plant innate immune system: structure, functions, and applications, Acta Nat. 8 (2016) 47–61. doi:10.32607/20758251-2016-8-2-47-61.
[53] P. Dubiela, R. Aina, D. Polak, S. Geiselhart, P. Humeniuk, B. Bohle, M. Bublin, K. Hoffmann-Sommergruber, S. Alessandri, R. Del Conte, F. Cantini, T. Borowski, Enhanced Pru p 3 IgE-binding activity by selective free fatty acid-interaction, J. Allergy Clin. Immunol. 140 (2017) 1728–1731.e10. doi:https://doi.org/10.1016/j.jaci.2017.06.016.
[54] J.P. Douliez, T. Michon, D. Marion, Steady-state tyrosine fluorescence to study the lipid-binding properties of a wheat non-specific lipid-transfer protein (nsLTP1), Biochim. Biophys. Acta Biomembr. 1467 (2000) 65–72. doi:https://doi.org/10.1016/S0005-2736(00)00197-8.

[55] C. Pato, M. Le Borgne, G. Le Baut, P. Le Pape, D. Marion, J.P. Douliez, Potential application of plant lipid transfer proteins for drug delivery, Biochem. Pharmacol. 62 (2001) 555–560, https://doi.org/10.1016/S0006-2952(01)00708-0.
[56] S. Schülke, Stephan Scheurer, Interaction of non-specific lipid-transfer proteins with plant-derived lipids and its impact on allergic sensitization, Front. Immunol. 9 (2018), https://doi.org/10.3389/fimmu.2018.01389.
[57] E. Johan, K. Blomqvist, N. Jeroen, T.A. Salminen, Plant lipid transfer proteins: are we finally closing in on the roles of these enigmatic proteins? J. Lipid Res. 59 (2018) 1374–1382, https://doi.org/10.1194/jlr.R083139.
[58] D.V. Lynch, T.M. Dunn, An introduction to plant sphingolipids and a review of recent advances in understanding their metabolism and function, New Phytol. 161 (2004) 677–702, https://doi.org/10.1111/j.1469-8137.2004.00992.x.
[59] S.S. Yeon, K.Y. Jung, N.M. Hee, P.K. Young, Phytosphingosine induces systemic acquired resistance through activation of sphingosine kinase, BioRxiv (2020), https://doi.org/10.1101/2020.05.08.084657.
[60] M. Duran-frigola, E. Pauls, O. Guitart-pla, M. Bertoni, V. Alcalde, D. Amat, T. Juan-blanco, P. Aloy, Extending the small-molecule similarity principle to all levels of biology with the chemical checker, Nat. Biotechnol. 38 (2020) 1087–1096, https://doi.org/10.1038/s41587-020-0502-7.
[61] J.M. Kulinski, R. Muñoz-cano, A. Olivera, Sphingosine-1-phosphate and other lipid mediators generated by mast cells as critical players in allergy and mast cell function, Eur. J. Pharmacol. (2015) 1–12, https://doi.org/10.1016/j.ejphar.2015.02.058.
[62] M. Mehrdad, C.G. Lo, G. Cinamon, M.J. Lesneski, Y. Xu, V. Brinkmann, M. L. Allende, R.L. Proia, J.G. Cyster, Lymphocyte egress from thymus and peripheral lymphoid organs is dependent on S1P receptor 1, Nature. 427 (2004) 355–360, https://doi.org/10.1038/nature02284.
[63] E. Fuerst, H.R. Foster, J.P.T. Ward, C.J. Corrigan, D.J. Cousins, G. Woszczek, Sphingosine-1-phosphate induces pro-remodelling response in airway smooth muscle cells, Allergy. 69 (2014) 1531–1539, https://doi.org/10.1111/all.12489.
[64] W.P. A, A. Aladhami, A.P. Chumanevich, J.W. Fuseler, C.A. Oskeritzian, Mast cells and sphingosine-1-phosphate underlie prelesional remodeling in a mouse model of eczema, Allergy. 73 (2018) 405–415, https://doi.org/10.1111/all.13310.
[65] Y.A. Hannun, L.M. Obeid, Sphingolipids and their metabolism in physiology and disease, Nat. Rev. Mol. Cell Biol. 19 (2017) 175–191, https://doi.org/10.1038/nrm.2017.107.